

Representation of auditory signals by neuronal spike trains

Bachelor project report

Maëlle Colussi

Computational Neuroscience Laboratory (LCN) - EPFL

Responsible professor: Prof. Wulfram Gerstner, Responsible assistant : Moritz Deger

1. Introduction

The neuronal representation of sound is the result of the encoding of acoustic signals by the peripheral auditory system. The spike trains resulting from this encoding are influenced, among other factors, by the refractory period of the auditory nerve fibers. In fact, for example we learn in [Avissar et al. 2013] that, for the encoding of pure tones, the spike timing precision depends on the ratio of the refractory period to the stimulus period, and the entrainment of nerve responses to the stimulus was better with the refractory period. We also know from [Berry and Meister 1998] that the refractoriness of neurons may make their signals more reliable.

This project aims to study the effects of refractoriness on sound encoding in the peripheral auditory system. First, we studied this effect based on an ad-hoc measure of response spike trains, the rate-modulation depth, for four kinds of stimuli. In [Deger et al. 2010], point processes with refractoriness were studied and mathematical predictions were made for the Fourier coefficients of their response. The second part of the project consisted on trying to see if the results on the model matches these predictions when the stimulus is a modulated pure tone.

For this aim, a model of the peripheral auditory system was used [Zilany and Bruce 2006, 2007; Zilany et al. 2009], in which the absolute refractory period has been modified. Virtual experiments were run on the two versions of the model and the resulting spike trains were compared to see the influence of the refractory period.

Now, before going any deeper into the model, we should introduce the basic physiology of the peripheral auditory system.

2. The Auditory System

This introduction is based on the book "Auditory Neuroscience" [Schnupp et al. 2011], chapter two.

The peripheral auditory system has (generally air) pressure as input, and spike trains as output. We will go through the parts of the ear, with help of Figure 1.

Let us first consider the external ear. There the pressure signals enters through the ear canal and make the eardrum vibrate. This takes to the medium ear, through which the vibration is propagated by three ossicles : malleus, incus and stapes. The farthest part from the external ear of the stapes touches the boundary of the cochlea, on the oval window, in the inner ear, and causes vibration in the contained liquid we find in it. The cochlea forms an interface between this mechanical vibration and the neural signal of the auditory nerve (VIII nerve on Figure 1).

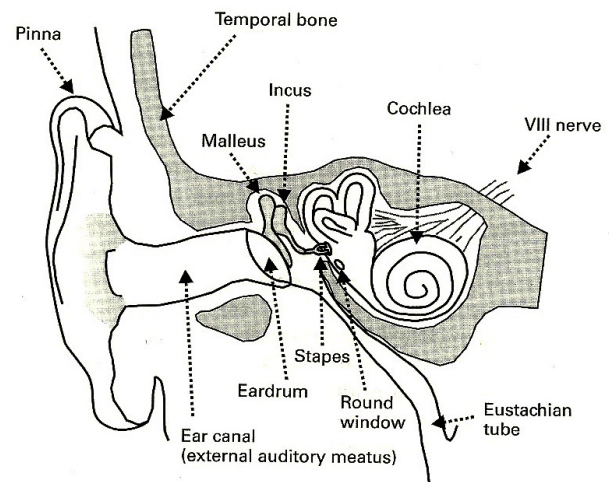


Figure 1. Peripheral auditory system ([Schnupp et al. 2011] p.52)

We will speak more about this interface below. But first we take a closer look at the vibration of the

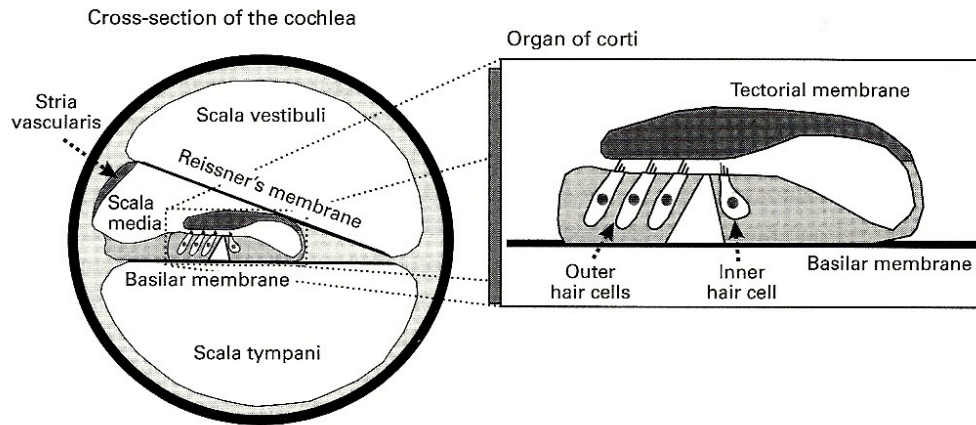


Figure 2. Organ of Corti ([Schnupp et al. 2011] p.65)

cochlea. The cochlea is a tube that has two main compartments which are placed on top of each other. These compartments are separated throughout the cochlear tube by the basilar membrane, except at the far end of it where they are joined, as can be seen on Figure 3.

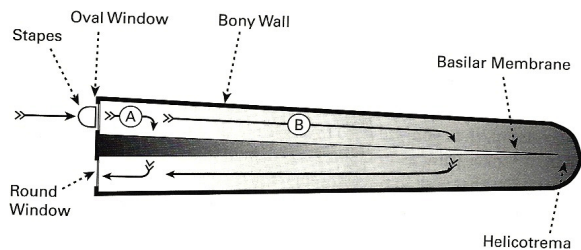


Figure 3. Unrolled cochlea ([Schnupp et al. 2011] p.55)

An incoming vibration will propagate through the basilar membrane from the upper compartment to the lower. In this process, it will not make all the parts of the basilar membrane vibrate at the same intensity. In fact, the cochlea is like a "biological Fourier analyzer". The frequency content of vibrations is decomposed and each frequency has its "favorite" place in the cochlear coiled tube that it makes vibrate particularly. The part of the basilar membrane that is the first to vibrate, when we gradually put on the volume of a pure tone of frequency f , is said to be of "characteristic frequency" f . Near the oval window, the characteristic frequencies are high, and as we advance to the tip of the tube, the characteristic frequency decreases.

Throughout the cochlear tube spans the organ of Corti, which is the interface which was previously ref-

ered to above in the text. We will use Figure 2 to illustrate its purpose.

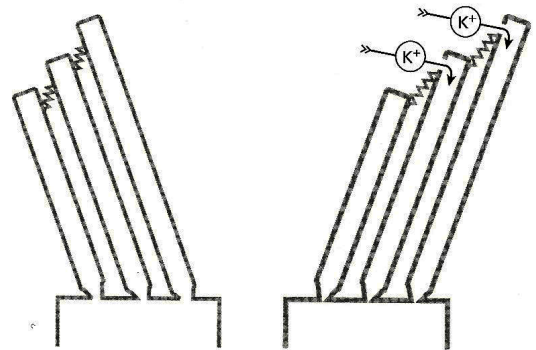


Figure 4. Transduction ([Schnupp et al. 2011] p.66)

The upper compartment of the cochlea is in fact in two parts separated by a membrane. The scala media, where we find the organ of Corti, has a higher concentration of potassium cations. A consequence, then is a polarization between the liquid of the scala media and the inner hair cells. When the basilar membrane vibrates, the tectorial membrane does that also, and that makes the liquid move. These movements cause the deflection of the stereocilia of the inner hair cells, and when this happens, some potassium ions of the scala media go into the inner hair cells (IHC), where they lead to a depolarization. This is depicted in Figure 4. This depolarization causes glutamate to be released at the synapses between the IHC and the auditory nerve fibers, what excites these fibers and make them emit action potentials (spikes).

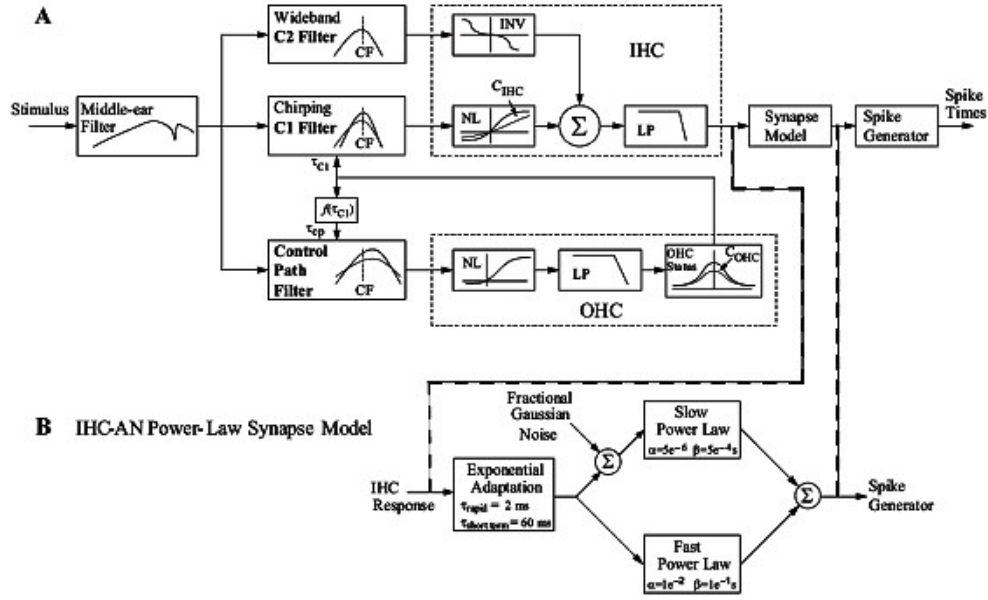


Figure 5. Schema of the model ([Zilany et al. 2009] their fig. 2)

3. Model

Let us now introduce the model of the peripheral auditory system [Zilany and Bruce 2006, 2007; Zilany et al. 2009], which was used to run experiments in this project.

We will not go into the details of the model, but from the use of it. You can see in Figure 5 the schematic of the model. It is a complicated cascade of linear and non-linear filters.

From the user point of view, the model consists of two main functions that are called "catmodel_IHC" and "catmodel_Synapse". Their prototype is

```
vihc = catmodel_IHC(pin, CF, nrep, tdres,
reptime, coh, cihc);
```

and

```
[synout, psth] = catmodel_Synapse(vihc,
CF, nrep, tdres, fibertype, implnt);
```

like specified in the "catmodel.m" file of the model.

Let us go deeper into what each parameter and return value of these functions means.

The first function, `catmodel_IHC`, takes as parameters a sound pressure stimulus vector (`pin`, in Pa), sampled at some sampling rate that is the inverse of the bin size specified in `tdres`, and the characteristic frequency (`CF`, in Hz) of the IHC and for which we want to know the potential (`vihc`, in Volt) when stimulated. This latter (`vihc`) is what is returned by the function. `reptime` is the time for one repetition of the stimulus,

and `nrep` is the number of repetitions we want to be run. The parameters `coh` and `cihc` represents the damages on respectively the outer hair cells and inner hair cells in the simulation (not used in this project). `vihc` will contain the IHC potential for every repetition after the function has been run.

The second function, `catmodel_Synapse`, takes the IHC potential returned by `catmodel_IHC`, with the same sampling rate, so the same `tdres`, which is also here the bin size of the PSTH returned by the function (`psth`). The PSTH will be computed according to the specified number of repetitions (`nrep`). The synapse output of the IHC (`synout`) is also returned by the function. The `fibertype` parameter is used to tell the model which nerve fiber type we "test" with the stimulus, distinguished by their spontaneous rate (SR) : low, medium or high. Finally, `implnt` is used to indicate the precision we want in the simulation for the power-law functions in the model.

As an example of what kind of result the model can give, in Figure 6 you can see some graphs that represents the steps of a simulation of a pure tone step stimulus. A nerve fiber with high SR with a 1 kHz characteristic frequency was chosen.

The first graph is a representation of one period of the stimulus, sampled at 100'000 Hz (so with bins of 0.01 ms size), at 84dB SPL. The stimulus, as given to the model as `pin`, was this period of 100 ms repeated

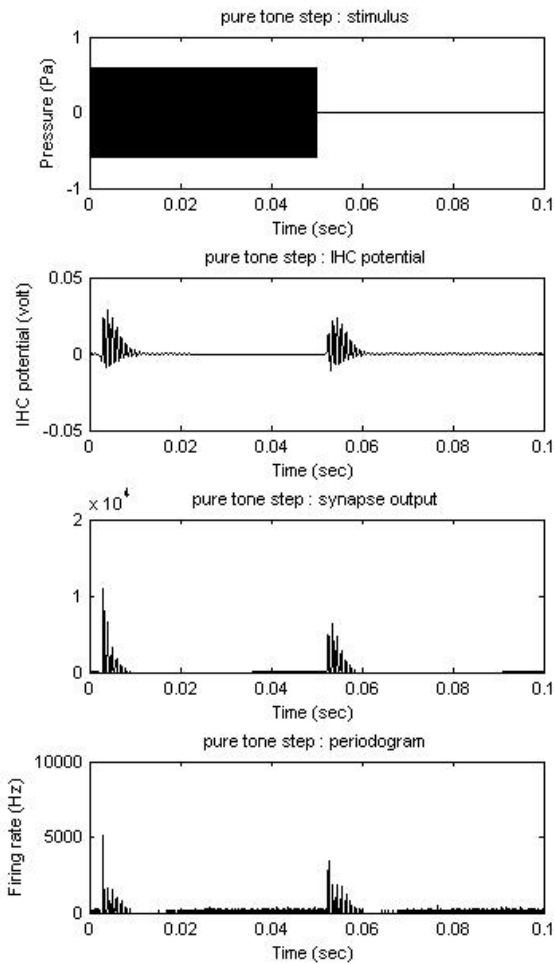


Figure 6. Example of model results ([Zilany et al. 2009])

800 times : a pure tone step. The frequency of the pure tone is so high here (10 kHz) that we cannot see its sinusoid. On the second graph, you can see the IHC potential from the first function in response of the last repetition of the stimulus (with dependencies on the preceding periods included). The third graph shows a part of the synapse output given by `catmodel.Synapse`, for the same period as for the potential of IHC. The fourth graph represents the peristimulus time histogram (PSTH).

For the project, the code of the model has been modified to put to zero the absolute refractory period (ARP) of nerve fibers. This transformation was done in the spike generator part of the model (see in Figure 5 the

last step on the right). After that, the spike trains with and without this refractory period could be compared.

In Figure 7 you can see an example of a graph where are drawn two periodograms, calculated from the PSTH given by the model (either modified or not), for another stimulus as before, a pure tone which is not modulated.

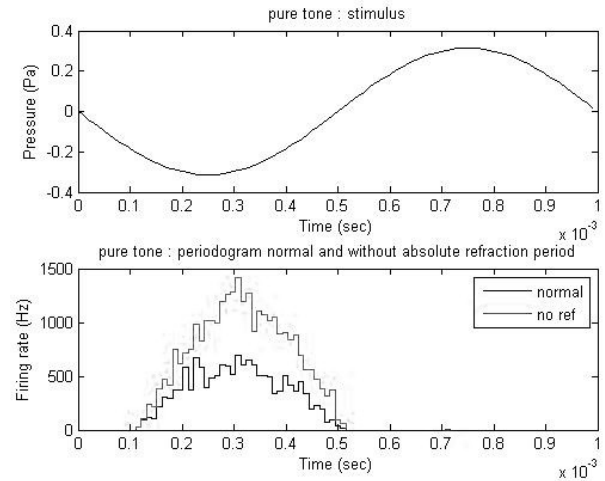


Figure 7. Periodogram with and without refractory period for the stimulus of period above

In Figure 7, first graph, you can see one period of the stimulus, a 1 kHz pure tone, at 84dB SPL. The second graphs shows the periodogram with and without absolute refractory period. We can see phase-locking for the two periodograms : spikes occur preferentially for a specific phase of the stimulus cycle. We see that here the phase characteristics seems not to change when the refractory period changes. This simulation was done with a medium SR nerve fiber, with 1 kHz characteristic frequency and 100 ms bin size. We will see now describe the results of the project.

4. Results

4.1 Rate modulation depth

For the first part of the project, an ad-hoc measure called rate modulation depth (RMD) was used to quantify differences between encoding of acoustic signal with and without an absolute refractory period (ARP) of the auditory nerve.

Four kinds of experiments were run and the average RMD was calculated for each of them, with each type of nerve fiber, and three different sound intensities : 49dB SPL, 84dB SPL and 120dB SPL (49 dB : average

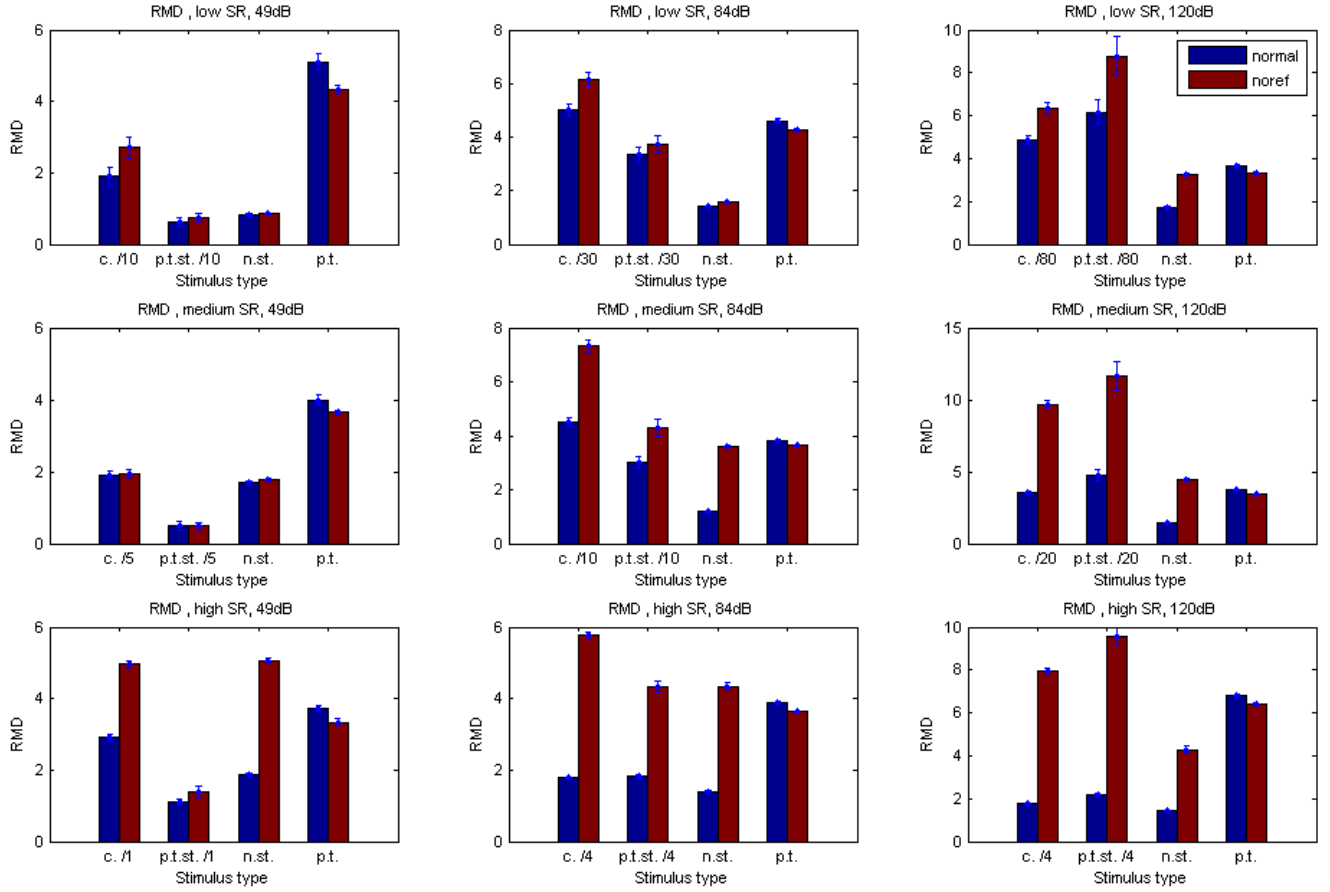


Figure 8. RMD values for different SR fibers and intensities. Experiments are abbreviated (c. for click, p. t. st. for pure tone step, n. st. for noise step, p. t. for pure tone). Some RMD results had to be scaled to fit properly in the graph and the scaling factor is written in the legend of the x-axis. From left to right, we have sound intensities : 49 dB, 84 dB, 120 dB, from top to bottom, we have fiber types : low SR, medium SR and high SR

home, rainfall; 84 dB : busy road; 120 dB : threshold of discomfort, possible hearing loss) to have an overall view of the effects. For each virtual experiment, the bin size was 0.01 ms, the characteristic frequency was 1 kHz, there was no damage on IHC or OHC, and we told the model to use the built-in approximations for power-law function calculations.

The four experiments were clicks, pure tones, noise steps and pure tone steps. The clicks were rarefaction clicks (negative pressure excursion) of 0.1 ms and sufficient time was waited between two of them to avoid influence from one to the other. The two step stimuli had a period of 100 ms and in the first half of the period there was noise or pure tone signal, and in the second half there was 0 Pa as pressure. The noise for the noise step was composed of random normal variables

divided by the square root of the bin size (gaussian white noise). The pure tone of the pure tone step was of 10kHz frequency.

The rate modulation depth (RMD) was defined as

$$RMD = (max - baseline)/baseline \quad (1)$$

where max was the maximum of the periodogram of the encoded sounds when converted in 2 ms bins. The meaning of the baseline depended on the stimulus. For the clicks it corresponded to the mean response to a 0 Pa pressure signal, with same number of repetitions than for the click stimulus. For the noise step, the baseline is the value of the periodogram just before the second half of the period, so just before the stimulus onset,

in 10 ms bins. The baseline for the pure tone step was the mean of periodogram values of a response to a pure tone of the frequency used for the stimulus (10 kHz), after the IHC were saturated (as could be seen in the potential, which stays constant because it has not the time to be depolarized between two periods of the stimulus). The periodogram was computed from the same number of repetitions as for the other stimuli, like for the click baseline. For the pure tone, the baseline was chosen as the mean of the periodogram.

Figure 8 displays RMD values as obtained in our virtual experiments, for several fiber types and sound intensities. As displayed on this figure, for each type of nerve fiber and each decibel value experimented we have similar effects in the following sense : for clicks, pure tone steps and noise steps, the RMD without absolute refractory period is bigger than for the normal case, and it is the opposite for pure tones.

We may explain the first finding because, first, we are in presence of a highly non-linear system and, secondly, the three stimuli for which the RMD without ARP is bigger, are stimuli with very sudden changes. In fact, the click can be seen as an approximation of a delta function, which corresponds to a broad-band stimulus. Also, sudden steps excite a wide range of frequencies, which make many non-linearities of the system contribute to the response.

The second fact, the fact that RMD is lower for pure tones without ARP, corresponds to what can be explain by the fact that we have less interactions between frequencies in non-linear system, and with ARP, we have a more non-linear system.

4.2 Response according to frequencies of modulated pure tones

In [Deger et al. 2010], predictions are made for the absolute value (norm) and angle of the Fourier coefficients (harmonics 0, 1, 2 and 3) of response of stochastic point processes with refractory period, to pure tone stimuli, as a function of the frequency. This case roughly corresponds to a tone with a high frequency carrier function, modulated by a low frequency oscillation. In fact, the inner hair cells will not be able to follow the carrier frequency and they will excite the nerve with a synaptic release rate dominated by the modulation.

In fact, the product of the absolute refractory period d and the modulation frequency f , determines the re-

sponse spectrum, as shown in Figure 9 (norm of Fourier coefficient) and Figure 10 (angle). Here d was 80 ms. In the graphs, the black ligns are for harmonic 0, dark gray for 1, mid gray for 2, light gray for 3. β_k is defined as

$$\beta_k = \sum_{l=-\infty}^{\infty} \alpha_{k-l} \Lambda_l \quad (2)$$

where the α_k are the Fourier coefficients for the active fraction of component processes with age $\theta \geq d$, and the Λ_k are the Fourier coefficients for the stimulus.

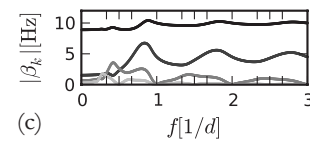


Figure 9. Predictions for norm ([Deger et al. 2010] their fig. 3 (c))

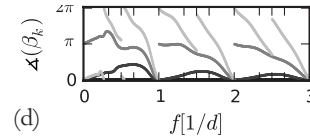


Figure 10. Predictions for angle ([Deger et al. 2010] their fig. 3 (d))

To see if the predictions are coherent with the model of the peripheral auditory system, experiments with modulated pure tone were run. The carrier frequency used was 10 kHz, the modulation frequency varied from 50 Hz to 4000 Hz with steps of 50 Hz. We chose nerve fibers with medium SR, and the stimuli were of intensity 84 dB. Sadly, not enough data could be yet calculated to see if the results match the predictions of [Deger et al. 2010].

5. Conclusion

The rate modulation depth calculation gave interesting results. In fact, RMD is a measure of the relative precision of response, and we found that absolute refractory period increased precision only for a specific stimulus (pure tone), but not generally. This result comes in contrast to generalizations of [Berry and Meister 1998].

For the second part of the project, more data should be calculated to conclude anything.

References

- M. Avissar, J. H. Wittig, Jr, J. C. Saunders, and T. D. Parsons. Refractoriness Enhances Temporal Coding by Auditory Nerve Fibers. *The Journal of Neuroscience* 33, 18:7681–7690, 2013.
- M. J. Berry and M. Meister. Refractoriness and Neural Precision. *The Journal of Neuroscience* 18, pages 2200–2211, 1998.
- M. Deger, M. Helias, S. Cardanobile, F. M. Atay, and S. Rotter. Nonequilibrium dynamics of stochastic point process with refractoriness. *Physical Review E* 82, 2010.
- J. Schnupp, I. Nelken, and A. King. *Auditory Neuroscience - Making Sense of Sound*. The MIT Press, 2011.
- M. S. A. Zilany and I. C. Bruce. Modeling auditory-nerve responses for high sound pressure levels in the normal and impaired auditory periphery. *Journal of the Acoustical Society of America* 120, 3:1446–1466, 2006.
- M. S. A. Zilany and I. C. Bruce. Representation of the vowel /eh/ in normal and impaired auditory nerve fibers: Model predictions of responses in cats. *Journal of the Acoustical Society of America* 122, 1:402–407, 2007.
- M. S. A. Zilany, I. C. Bruce, P. C. Nelson, and L. H. Carney. A phenomenological model of the synapse between the inner hair cell and auditory nerve: Long-term adaptation with power-law dynamics. *Journal of the Acoustical Society of America* 126, 5:2390–2412, 2009.